

Structural, Magnetic, and Charge Transport Properties of Bis[(5,10,15,20-tetramethylporphyrinato)palladium(II)] Perrhenate, [Pd(tmp)]₂[ReO₄]

Ellen M. McGhee, Brian M. Hoffman,* and James A. Ibers*

Received September 13, 1990

Electrochemical oxidation of (5,10,15,20-tetramethylporphyrinato)palladium(II), Pd(tmp), in the presence of the perrhenate ion affords the new molecular conductor [Pd(tmp)]₂[ReO₄]. The compound is composed of partially oxidized (+1/2) Pd(tmp) cations stacked metal-over-metal (Pd-Pd_{av} = 3.373 (4) Å) and surrounded by chains of ReO₄ anions. Single-crystal room-temperature conductivity along the needle (crystallographic *c*) axis averages 30 Ω⁻¹ cm⁻¹ and may be fit to an expression that describes a semiconductor with temperature-dependent carrier mobility, $\sigma = \sigma_0 T^{-\alpha} \exp(-\Delta E/k_B T)$ ($\Delta E = 0.10$ (2) eV; $\alpha = 2.2$ (5)). ESR measurements confirm the tmp ligand as the site of oxidation. The compound crystallizes in space group C_{4h}^3-P4/n of the tetragonal system with two formula units in a cell of dimensions $a = 16.778$ (6) Å and $c = 6.723$ (3) Å ($V = 1892$ Å³) at 110 K. Full-matrix least-squares refinement of 67 variables gives a final value of 0.187 for the *R* index on F^2 for 2404 unique observations and a value of 0.090 for the *R* index on *F* for the 1179 observations having $F_o^2 > 3\sigma(F_o^2)$.

Introduction

Electronic conduction in partially oxidized systems such as K₂[Pt(CN)₄]Cl_{0.32}·2.6H₂O¹ occurs through chains of metal atoms separated by ~2.88 Å.^{1a,b} Platinum is particularly suited for this type of conduction because of the propensity for third-row transition metals to form M-M bonds. Third-row transition metals are also more likely to form clusters; these frequently have shorter M-M bonds than are found with first- and second-row metals. This propensity for conduction through the chains of third-row metals results, in part, from the fact that the required spatial extension of the bond-forming molecular orbitals is proportional to the principal quantum number.² For square-planar inorganic transition-metal complexes, the extension increases as 3d_z << 4d_z < 5d_z. The greater spatial extension of the 5d_z orbitals yields greater overlap, stronger interactions, and shorter bond lengths, balancing the effect of the greater atomic radii of the third-row transition metals. Palladium complexes with M-M bonds are known,³ but they are not as numerous as those of platinum, consistent with the trends just described. To date, no partially oxidized palladium complexes with metallic conduction, analogous to the tetracyanoplatinate salts, have been synthesized.

In contrast, Ni(pc)I_{1.0}, Pd(pc)I_{1.0}, and Pt(pc)I_{1.36} have been synthesized and found to conduct electricity through the aromatic π-electron system of the ligand.⁴ The order of their room-temperature conductivities (Ni σ_{RT} = 750 Ω⁻¹ cm⁻¹, Pd σ_{RT} = 340 Ω⁻¹ cm⁻¹, Pt σ_{RT} = 200 Ω⁻¹ cm⁻¹) is consistent with the trend in atomic number, atomic mass, and electronegativity, but the differences are not large. The metal-d_z orbital overlap might be expected to increase across this series as a result of the increasing spatial extension, but the shortest metal-metal distance allowed by the ligand π-orbitals is ~3.2 Å. The conductivity of the inorganic platinum complexes decreases dramatically when the Pt-Pt distance exceeds ~2.9 Å.¹ Thus, the metal contribution to the conductivity of the phthalocyanine salts is negligible even for the largest cation, Pt(II).

Table I. Crystal Data and Experimental Details for [Pd(tmp)]₂[ReO₄]

compd	bis[(5,10,15,20-tetramethylporphyrinato)palladium(II)] perrhenate
formula	C ₄₈ H ₄₀ N ₈ O ₄ Pd ₂ Re
fw	1191.91
cell const	
<i>a</i> , Å	16.778 (6)
<i>c</i> , Å	6.723 (3)
<i>V</i> , Å ³	1892
<i>Z</i>	2
temp, K	110 ^a
<i>d</i> _{calc} , g/cm ³	2.091
space group	C_{4h}^3-P4/n
radiation	Mo Kα graphite-monochromated (λ(Kα ₁) = 0.7093 Å)
μ, cm ⁻¹	42.2
transm coeff ^b	0.777-0.815
<i>R</i> on F_o^2	0.187
<i>R</i> _w on F_o^2	0.204
<i>R</i> on F_o with $F_o^2 > 3\sigma(F_o^2)$	0.090

^aThe low-temperature system is based on a design by: Huffman, J. C. Ph.D. Thesis, Indiana University, 1974. ^bThe analytical absorption correction was performed with the use of the Northwestern absorption program AGNOST. See: de Meulenaer, J.; Tompa, H. *Acta Crystallogr.* **1965**, *19*, 1014-1018.

Reported here are the synthesis and characterization of the partially oxidized porphyrin molecular conductor [Pd(tmp)]₂[ReO₄]. We have previously reported the synthesis and characterization of [Ni(tmp)]₂[ReO₄]⁵ and [Cu(tmp)]₂[ReO₄],⁶ which are ligand-based conductors, in analogy to the iodine-oxidized M(pc) systems, M = Ni, Pd, and Pt. The structure and properties of the present Pd complex are completely analogous to those of the corresponding Ni complex.

Experimental Section

Preparation of [Pd(tmp)]₂[ReO₄]. Free-base 5,10,15,20-tetramethylporphyrin, H₂(tmp), was prepared as described elsewhere.^{6,7} Metalation of H₂(tmp) (200 mg) with palladium(II) chloride (200 mg) was performed in *N,N*-dimethylformamide (500 mL) at 90 °C for 1 h. Pd(tmp) was extracted into CHCl₃ and chromatographed through silica and alumina columns to afford the optically pure product.

Black rectangular needles of [Pd(tmp)]₂[ReO₄] were crystallized at a platinum-wire electrode by constant-current (2 μA) electrolysis of a CH₂Cl₂ solution containing [N(*n*-Bu)₄][ReO₄] (1.5 × 10⁻² M) and saturated with Pd(tmp). Elemental analysis was carried out by

- (1) (a) Krogmann, K.; Hausen, H. D. *Z. Anorg. Allg. Chem.* **1968**, *358*, 67-81. (b) Krogmann, K. *Angew. Chem.* **1969**, *8*, 35-42. (c) Thomas, T. W.; Underhill, A. E. *Chem. Soc. Rev.* **1972**, *1*, 99-120. (d) Underhill, A. E. *Platinum Met. Rev.* **1974**, *18*, 21-26. (e) Underhill, A. E.; Wood, D. J. *Ann. N.Y. Acad. Sci.* **1978**, *313*, 516-524. (f) Underhill, A. E.; Watkins, D. M. *Chem. Soc. Rev.* **1980**, *9*, 429-448. (g) Zeller, J. R.; Beck, A. J. *Phys. Chem. Solids* **1974**, *35*, 77-80. (h) Williams, J. M.; Schultz, A. J. *Ann. N.Y. Acad. Sci.* **1978**, *313*, 509-515. (i) Krogmann, K.; Stephan, D. Z. *Anorg. Allg. Chem.* **1968**, *362*, 290-300. (j) Williams, J. M.; Petersen, J. L.; Gerdes, H. M.; Peterson, S. W. *Phys. Rev. Lett.* **1974**, *33*, 1079-1081.
- (2) Miller, J. S. *Ann. N.Y. Acad. Sci.* **1978**, *313*, 25-59.
- (3) (a) Boehm, J. R.; Balch, A. L. *Inorg. Chem.* **1977**, *16*, 778-785. (b) Holloway, R. G.; Penfold, B. R.; Colton, R.; McCormick, M. J. *J. Chem. Soc., Chem. Commun.* **1976**, 485-486.
- (4) Hoffman, B. M.; Martinsen, J.; Pace, L. J.; Ibers, J. A. In *Extended Linear Chain Compounds*; Miller, J. S., Ed.; Plenum Press: New York, 1981, pp 459-549. (b) Schramm, C. J. Ph.D. Thesis, Northwestern University, 1979.

- (5) Newcomb, T. P.; Godfrey, M. R.; Hoffman, B. M.; Ibers, J. A. *Inorg. Chem.* **1990**, *29*, 223-228.
- (6) McGhee, E. M.; Godfrey, M. R.; Hoffman, B. M.; Ibers, J. A. *Inorg. Chem.* **1991**, *30*, 803-808.
- (7) (a) Ulman, A.; Gallucci, J.; Fisher, D.; Ibers, J. A. *J. Am. Chem. Soc.* **1980**, *102*, 6852-6854. (b) Ulman, A.; Fisher, D.; Ibers, J. A. *J. Heterocycl. Chem.* **1982**, *19*, 409-413.

Schwarzkopf Microanalytical Laboratory, Woodside, NY, and is consistent with the formula [Pd(tmp)]₂[ReO₄]. Anal. Calcd for C₄₈H₄₀N₈O₄Pd₂Re: C, 48.37; H, 3.38; N, 9.40. Found: C, 47.35; H, 3.40; N, 9.29.

Visible Spectroscopy. Electronic spectra between 350 and 800 nm were recorded on a Hewlett Packard (8452A) diode-array spectrophotometer. Spectra were taken of the M(tmp) complexes in CHCl₃ solutions.

X-ray Diffraction Study of [Pd(tmp)]₂[ReO₄]. We have previously reported two isostructural compounds of the formula [M(tmp)]₂[ReO₄] (M = Ni, Cu).^{5,6} Weissenberg photographs of [Pd(tmp)]₂[ReO₄] are superimposable on those of the Cu and Ni analogues. These compounds crystallize in space group C_{2h}²-P4/n of the tetragonal system. Crystals of the present Pd compound were of marginal quality, as judged by the photographs and by preliminary ω -scans. The cell constants were determined by a least-squares refinement of the setting angles of 15 reflections that had been centered on a Picker FACS-I diffractometer. Intensity data were collected at 110 K with the θ -2 θ scan technique.⁸ No systematic changes were seen in the six standard reflections that were measured every 100 reflections. Experimental details and crystal data are found in Table I; more information is available in Table IS.⁹

After correction for absorption the data equivalent in 4/m were averaged ($R_w = 0.087$). Initial refinement was on F_o with the 1179 unique reflections having $F_o^2 > 3\sigma(F_o^2)$. All non-hydrogen atomic positions from the [Cu(tmp)]₂[ReO₄] structure were used as the starting values. Least-squares refinement on F_o with isotropic thermal parameters of all non-hydrogen atoms led to a value for the R index of 0.12. Possibly because of the poor quality of the crystal and hence of the resultant data set, but certainly not because of the absorption correction, upon a change to anisotropic thermal parameters the refinement gave nonpositive definite thermal ellipsoids for some of the atoms of the cation. In subsequent calculations only the Re atom was allowed to vibrate anisotropically. Most of the hydrogen atom positions were determined from a difference electron density map, but in successive refinements their positions were idealized (C-H = 0.95 Å) and held constant. Each hydrogen atom was given an isotropic thermal parameter 1 Å² larger than that of the carbon atom to which it is bonded. The final refinement on F_o^2 converged to $R(F^2) = 0.187$ for all 2404 observations, including $F_o^2 < 0$, and 67 variables. The value of $\sum w(F_o^2 - F_c^2)^2$ as a function of $\lambda^{-1} \sin \theta$, F_o^2 , and setting angles showed no unusual trends. A final difference electron density map shows peaks as large as 7.5 e/Å³ ~ 0.5 Å from the perchinate anion but is otherwise featureless. The typical peak height of a carbon atom is 13 e/Å³. The final positional and isotropic thermal parameters are given in Table II. Table IIS provides a listing of $10|F_o|$ vs $10|F_c|$.⁹

Single-Crystal Electrical Conductivity Measurements. The single-crystal electrical conductivity of [Pd(tmp)]₂[ReO₄] was measured along the needle (c) axis with the use of a four-probe ac (27 Hz) phase-locked technique, as described elsewhere.¹⁰ The sample dimensions ranged from 0.1 to 0.2 mm in length and 4×10^{-4} to 3×10^{-3} mm² in cross-sectional area. The uncertainties in the measurements of these dimensions lead to $\Delta(\sigma)/\sigma = \pm 0.2$. These needle-shaped crystals are too thin to enable the measurement of conductivity perpendicular to the needle axis.

Electron Spin Resonance Measurements. Powder and single-crystal ESR spectra were obtained with a Bruker X-band (9.5 GHz) spectrometer with 100-kHz field modulation, as described previously.¹¹ The data were digitized and stored with the use of the program EPR Data Acquisition System.¹² The spin susceptibility, χ^s , was determined by double integration of the first-derivative ESR signal. Determination of the absolute spin concentration utilized [Ni(tmp)]₂[ReO₄] (0.031 spins per macrocycle) as a standard.⁷

Magnetic Susceptibility Measurements. The static magnetic susceptibility of [Pd(tmp)]₂[ReO₄] was determined at a field strength of 5 kG with a Quantum Design SQUID susceptometer. The background magnetic contribution of the sample holder was measured over the full temperature range. The sample weight was 47 mg.

Results and Discussion

Visible Spectroscopy. The d_{xz} and d_{yz} orbitals of the metal possess π -symmetry and may interact with the aromatic π -electron

Table II. Positional Parameters and Isotropic Thermal Parameters for [Pd(tmp)]₂[ReO₄]

atom	x	y	z	$B, \text{\AA}^2$
Re	1/4	3/4	1/2	1.86 (3) ^a
Pd(1)	1/4	1/4	0.37521 (47)	0.92 (4)
Pd(2)	-1/4	-1/4	0.12468 (47)	0.82 (4)
O	0.303 53 (78)	-0.183 77 (78)	0.3728 (26)	3.4 (4)
N(1)	0.143 44 (69)	0.194 97 (69)	0.3765 (24)	1.0 (2)
C(11)	0.127 10 (88)	0.114 26 (88)	0.3820 (29)	1.2 (3)
C(12)	0.043 39 (80)	0.101 50 (80)	0.3775 (29)	0.7 (2)
C(13)	0.007 30 (87)	0.171 61 (89)	0.3778 (31)	1.2 (3)
C(14)	0.069 57 (90)	0.232 64 (88)	0.3776 (30)	1.1 (3)
C(15)	0.185 42 (81)	0.055 31 (83)	0.3752 (28)	0.7 (2)
C(16)	0.159 96 (88)	-0.030 75 (89)	0.3744 (31)	1.2 (3)
N(2)	-0.178 79 (63)	-0.153 35 (63)	0.1265 (22)	0.4 (2)
O(21)	-0.200 07 (85)	-0.074 00 (86)	0.1295 (29)	1.0 (2)
C(22)	-0.131 51 (87)	-0.026 39 (86)	0.1294 (30)	1.1 (3)
C(23)	-0.068 07 (85)	-0.073 02 (86)	0.1205 (30)	1.0 (2)
C(24)	-0.095 46 (87)	-0.153 82 (88)	0.1269 (31)	1.2 (3)
C(25)	-0.045 89 (89)	-0.219 99 (87)	0.1244 (30)	1.1 (3)
C(26)	0.042 76 (90)	-0.205 87 (89)	0.1213 (31)	1.4 (3)
H1C(12)	0.018	0.051	0.375	1.7
H1C(13)	-0.049	0.181	0.379	2.2
H1C(22)	-0.131	0.030	0.135	2.1
H1C(23)	-0.014	-0.056	0.111	2.0
H1C(16)	0.116	-0.038	0.459	2.3
H2C(16)	0.145	-0.045	0.241	2.3
H3C(16)	0.203	-0.063	0.415	2.3
H1C(26)	0.062	-0.208	0.257	2.3
H2C(26)	0.068	-0.245	0.046	2.3
H3C(26)	0.053	-0.155	0.070	2.3

^aThis value is the equivalent isotropic thermal parameter, B_{eq} . For the Re atom, $U_{11} = U_{22} = 0.012 52$ (41) Å² and $U_{33} = 0.0458$ (11) Å².

system of the ligand.¹³ The effect of the metal atom on the electronic structure of the macrocycle may be seen in the shift of the π - π^* bands in the optical spectra of the unoxidized complexes. The Soret peaks of the M(tmp) series (M = Cu, Ni, Pd) do not differ significantly ($\lambda(\text{Cu}) = 418$ nm; $\lambda(\text{Ni}) = 419$ nm; $\lambda(\text{Pd}) = 418$ nm), but the α - β bands of this series are red shifted by an average of 9 nm ($\lambda(\text{Cu}) = 545$ (central peak), 512, and 584 nm (shoulders); $\lambda(\text{Ni}) = 539$ (central peak), 500, and 575 nm (shoulders); $\lambda(\text{Pd}) = 531$ (central peak), 492, and 564 nm (shoulders)).¹⁴ This effect is seen in the Cu, Ni, and Pd series of both the phthalocyanine and tetraphenylporphyrin systems.¹⁵

Description of the Structure. [Pd(tmp)]₂[ReO₄] is isostructural with [M(tmp)]₂[ReO₄], M = Cu⁶ and Ni,⁵ and hence, the description of its structure will be very brief. In all three systems the planar tmp cations form metal-over-metal stacks along the crystallographic c axis. These stacks contain two independent M(tmp) cations that are rotated by 26.3 (1)° (Pd(tmp)), 27.4 (1)° (Cu(tmp)), and 27.5 (1)° (Ni(tmp)) about the c axis with respect to one another. The tetrahedral ReO₄ anion lies on a site of crystallographically imposed $\bar{4}$ symmetry within the channels formed by the Pd(tmp) columns. The Pd-Pd spacings along a stack are the same within experimental error (Pd(1)-Pd(2) = 3.371 (5) Å and Pd(2)-Pd(1)' = 3.375 (4) Å). These values do not differ from those in the Cu system (Cu(1)-Cu(2) = 3.369 (1) Å and Cu(2)-Cu(1)' = 3.377 (1) Å) and are perhaps slightly longer than those in the Ni system (Ni(1)-Ni(2) = 3.355 (2) Å and Ni(2)-Ni(1)' = 3.365 (2) Å). The similar M-M distances for [M(tmp)]₂[ReO₄], M = Pd, Cu, and Ni, indicate that the

(8) Corfield, P. W. R.; Doedens, R. J.; Ibers, J. A. *Inorg. Chem.* **1967**, *6*, 197-204.

(9) Supplementary material.

(10) Phillips, T. E.; Anderson, J. R.; Schramm, C. J.; Hoffman, B. M. *Rev. Sci. Instrum.* **1979**, *50*, 263-265.

(11) Phillips, T. E.; Scaringe, R. P.; Hoffman, B. M.; Ibers, J. A. *J. Am. Chem. Soc.* **1980**, *102*, 3435-3444.

(12) Morse, P. D., II. EPR Data Acquisition System, Version 2.2. University of Illinois College of Medicine, Urbana, IL 61801.

(13) Schaffer, A. M.; Gouterman, M.; Davidson, E. R. *Theor. Chim. Acta* **1973**, *30*, 9-30.

(14) (a) Wolberg, A.; Manassen, J. *J. Am. Chem. Soc.* **1970**, *92*, 2982-2991. (b) Lever, A. B. P.; Licoccia, S.; Magnell, K.; Minor, P. C.; Ramaswamy, B. S. *Adv. Chem. Ser.* **1982**, *No. 201*, 237-252.

(15) (a) Edwards, L.; Dolphin, D. H.; Gouterman, M. *J. Mol. Spectrosc.* **1970**, *35*, 90-109. (b) Edwards, L.; Dolphin, D. H.; Gouterman, M.; Adler, A. D. *J. Mol. Spectrosc.* **1971**, *38*, 16-32. (c) Thomas, D. W.; Martell, A. E. *Arch. Biochem. Biophys.* **1958**, *76*, 286-294. (d) Williams, R. J. P. *Chem. Rev.* **1956**, *56*, 299-328. (e) Davis, D. G. In *The Porphyrins*; Dolphin, D., Ed.; Academic Press: New York, 1978; Vol. V, pp 127-152.

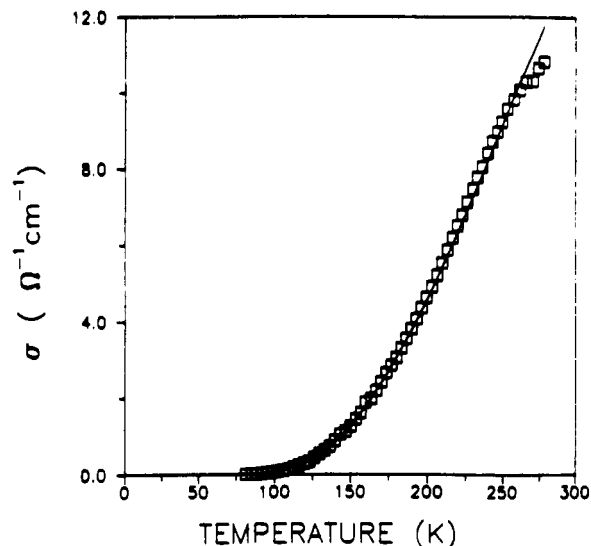


Figure 1. Conductivity along the needle *c* axis of $[\text{Pd}(\text{tmp})]_2[\text{ReO}_4]$ as a function of temperature.

intercation separation is determined by packing of the ligand.

Table IIIS⁹ summarizes the intramolecular bond distances and angles for $[\text{Pd}(\text{tmp})]_2[\text{ReO}_4]$; these are as expected. The Pd(tmp) cations are planar (maximum deviation 0.021 (2) Å), although this is not a crystallographically imposed condition. The best weighted least-squares planes are given in Table IVS.⁹

Single-Crystal Electrical Conductivity. The room-temperature conductivity of different $[\text{Pd}(\text{tmp})]_2[\text{ReO}_4]$ crystals ranges from 10 to 50 $\Omega^{-1} \text{cm}^{-1}$. The conductivity decreases with decreasing temperature in an activated fashion (Figure 1) and may be fit to the following expression with a thermally activated carrier mobility term:¹⁶

$$\sigma/\sigma_0 = T^{-\alpha} \exp(-\Delta E/k_B T) \quad (1)$$

where σ/σ_0 is the normalized conductivity, α is a mobility parameter, ΔE is the activation energy for conduction, and k_B is Boltzmann's constant. A least-squares fit of the data to eq 1 yields $\alpha = 2.2$ (5) and $\Delta E = 0.10$ (2) eV. These may be compared with $\alpha = 3.8$ (2) and $\Delta E = 0.126$ (2) eV for the Cu system and $\alpha = 11$ (7) and $\Delta E = 0.24$ (2) in the Ni system. Thus, the differences among these systems are minimal.

The metal ion appears to influence the conductivity indirectly in these compounds, but conduction through the metal ion orbitals is unlikely. The M–M distance, 3.373 (4) Å, is well within the distance for the semiconducting inorganic metal complexes (i.e., $\text{Sr}[\text{M}(\text{CN})_4] \cdot 5\text{H}_2\text{O}$, $\sigma_{\text{RT}} = 10^{-4} \Omega^{-1} \text{cm}^{-1}$, M–M = 3.64 (Ni), 3.63 (Pd), and 3.60 Å (Pt))^{16j} but is larger than the corresponding distance in the partially oxidized metallic conductors (i.e., $\text{K}_2[\text{Pt}(\text{CN})_4]\text{Br}_{0.3} \cdot 3\text{H}_2\text{O}$, $\sigma_{\text{RT}} = 10^2 \Omega^{-1} \text{cm}^{-1}$, Pt–Pt = 2.890 (2) Å).^{17j} For comparison, the Pt–Pt distance in Pt metal is 2.7746 (1) Å and $\sigma_{\text{RT}} = 10^5 \Omega^{-1} \text{cm}^{-1}$.¹⁷

Electron Spin Resonance Measurements. Single-crystal ESR studies of $[\text{Pd}(\text{tmp})]_2[\text{ReO}_4]$ show that this system possesses a single isotropic signal with $g = 2.000$ (1) at room temperature. Since this value is close to the free-electron g value (2.0023), the site of partial oxidation is exclusively the tmp ligand. We speculate that the $\approx 27^\circ$ twist angle between the macrocycles in $[\text{Cu}(\text{tmp})]_2[\text{ReO}_4]$, $[\text{Pd}(\text{tmp})]_2[\text{ReO}_4]$, and $[\text{Ni}(\text{tmp})]_2[\text{ReO}_4]$ not only decreases the overlap between the HOMO's of the macrocycles, reducing carrier mobility along the stacks, but also reduces the $d-\pi$ interactions, thus giving the isotropic g value seen in the Ni and Pd systems. In $[\text{Ni}(\text{tmp})]_2[\text{PF}_6]$ the twist angle is 34.7 (3)°, the carrier electrons are more mobile, greater $d-\pi$ mixing

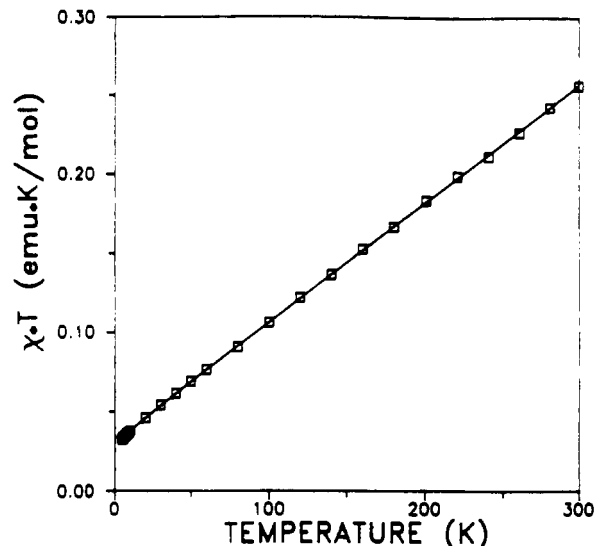


Figure 2. Temperature dependence of the paramagnetic susceptibility (χT).

occurs, and the g value exhibits an angular dependence.¹⁸ The room-temperature line width of $[\text{Pd}(\text{tmp})]_2[\text{ReO}_4]$, 13.5 (2) G, is larger than that of $[\text{Ni}(\text{tmp})]_2[\text{ReO}_4]$, 10.3 (2) G, while both are characteristic of π -radicals. Motional narrowing of the line width may be greater in the Ni system, which is a better conductor than $[\text{Pd}(\text{tmp})]_2[\text{ReO}_4]$. The opposite trend in line width with metal atom is seen in the phthalocyanine system ($\Gamma_0(\text{Ni}(\text{pc})\text{I}) = 3.6 \text{ G} > \Gamma_0(\text{Pd}(\text{pc})\text{I}) = 1.8 \text{ G}$).⁴), whose narrower lines reflect the higher conductivity of these compounds.

The g value does not change as the temperature is lowered to 77 K, but the line width decreases slightly to 9.7 (2) G. Similar changes in the line width with temperature are seen in $\text{Ni}(\text{pc})\text{I}$,¹⁹ $\text{Ni}(\text{tmp})\text{I}$,²⁰ $[\text{Ni}(\text{tmp})]_2[\text{ReO}_4]$,⁵ and $\text{Ni}(\text{omtpb})\text{I}_{1.08}$.²¹ In $\text{Ni}(\text{pc})\text{I}$ and $\text{Ni}(\text{tmp})\text{I}$ when the temperature is lowered, the carrier mobility increases and enhanced motional narrowing of the line width occurs. Enhanced motional narrowing cannot account for the decreasing line width in the semiconducting systems $[\text{Pd}(\text{tmp})]_2[\text{ReO}_4]$, $[\text{Ni}(\text{tmp})]_2[\text{ReO}_4]$, and $\text{Ni}(\text{omtpb})\text{I}_{1.08}$, where the conductivity decreases with decreasing temperature. An alternative explanation proposed for $\text{Ni}(\text{omtpb})\text{I}_{1.08}$ ascribes this behavior to the temperature dependence of correlated hopping of charge carriers.

The spin susceptibilities of the Pd and Ni systems display opposite trends with temperature. The spin susceptibility of $[\text{Ni}(\text{tmp})]_2[\text{ReO}_4]$ may be accounted for by 0.031 spins per macrocycle at room temperature and decreases by 65% as the temperature is lowered to 77 K. That of $[\text{Pd}(\text{tmp})]_2[\text{ReO}_4]$ may be accounted for by 0.041 spins per macrocycle and increases by a factor of 2.3 as the temperature is lowered to 77 K. This signal, which originates from unpaired electrons in the ligand π -orbitals, is weak in both of these systems. The different behavior may be ascribed to different concentrations of localized paramagnetic defect sites that may also be contributing to the ESR signal. Evidence for the presence of these sites has been found in the bulk magnetic susceptibility of $[\text{Ni}(\text{tmp})]_2[\text{ReO}_4]$ and $[\text{Cu}(\text{tmp})]_2[\text{ReO}_4]$.^{5,6}

(18) Newcomb, T. P.; Godfrey, M. R.; Hoffman, B. M.; Ibers, J. A. *J. Am. Chem. Soc.* **1989**, *111*, 7078–7084.

(19) (a) Schramm, C. J.; Scaringe, R. P.; Stojakovic, D. R.; Hoffman, B. M.; Ibers, J. A.; Marks, T. J. *J. Am. Chem. Soc.* **1980**, *102*, 6702–6713. (b) Martinsen, J.; Greene, R. L.; Palmer, S. M.; Hoffman, B. M. *J. Am. Chem. Soc.* **1983**, *105*, 677–678. (c) Martinsen, J.; Palmer, S. M.; Tanaka, J.; Greene, R. L.; Hoffman, B. M. *Phys. Rev. B: Condens. Matter* **1984**, *30*, 6269–6276.

(20) Pace, L. J.; Martinsen, J.; Ullman, A.; Hoffman, B. M.; Ibers, J. A. *J. Am. Chem. Soc.* **1983**, *105*, 2612–2620.

(21) (a) Phillips, T. E.; Hoffman, B. M. *J. Am. Chem. Soc.* **1977**, *99*, 7734–7736. (b) Hoffman, B. M.; Phillips, T. E.; Soos, Z. G. *Solid State Commun.* **1980**, *33*, 51–54. (c) Phillips, T. E.; Scaringe, R. P.; Hoffman, B. M.; Ibers, J. A. *J. Am. Chem. Soc.* **1980**, *102*, 3435–3444.

(16) (a) Kittel, C. *Introduction to Solid State Physics*; Wiley: New York, 1976. (b) Epstein, A. J.; Conwell, E. M.; Sandman, D. J.; Miller, J. S. *Solid State Commun.* **1977**, *23*, 355–358.

(17) Goldschmidt, H. J.; Land, T. J. *Iron Steel Inst.* **1947**, *155*, 221–226.

Bulk Susceptibility Measurements. The raw data ($\chi_{RT} = 3.58 \times 10^{-4}$ emu/mol) were corrected for temperature-independent diamagnetism ($\chi^d = -4.90 \times 10^{-4}$ emu/mol)²² to afford the paramagnetic susceptibility $\chi_{RT}^p = 8.54 \times 10^{-4}$ emu/mol. This value is significantly larger than that of $[\text{Ni}(\text{tmp})_2][\text{ReO}_4]$ ($\chi_{RT}^p = 2.49 \times 10^{-4}$ emu/mol). The temperature dependence of the susceptibility (Figure 2) may be fit to the Curie–Weiss expression with an added constant (Q), which accounts for the temperature-independent contribution to the susceptibility.

$$\chi^p = \frac{C}{T - \theta} + Q \quad (2)$$

A least-squares fit of the data yields $C = 3.18(1) \times 10^{-2}$ emu/mol K, $\theta = -0.60(1)$ K, and $Q = 7.50(1) \times 10^{-4}$ emu/mol. $[\text{Ni}(\text{tmp})_2][\text{ReO}_4]$ does not exhibit any Weiss constant, and the Curie constant ($C = 3.04(7) \times 10^{-3}$ emu/mol K) is 1 order of magnitude smaller than that in $[\text{Pd}(\text{tmp})_2][\text{ReO}_4]$. Scatter in the data for $[\text{Ni}(\text{tmp})_2][\text{ReO}_4]$ could account for the different Weiss constants in the Ni and Pd complexes. The number of localized noninteracting spin sites per mole (N) can be calculated from the expression for the Curie constant

$$C = S(S + 1)(Ng^2\beta^2/3k_B) \quad (3)$$

where β is the Bohr magneton, k is Boltzmann's constant, S is

(22) From Pascal's constants; see: (a) Drago, R. S. *Physical Methods in Chemistry*; W. B. Saunders: Philadelphia, PA, 1977; p 413. (b) Muly, L. N., Boudreaux, E. A., Eds. *Theory and Applications of Molecular Diamagnetism*; Wiley: New York, 1976; p 307.

the spin, and g is the Lande factor. The measured Curie constant corresponds to $N = 8.7 \times 10^{-2}$ spins per $\text{Pd}(\text{tmp})$ molecule that are assigned to impurities or defect sites. The value of the temperature-independent paramagnetism (Q) is larger than that in $[\text{Ni}(\text{tmp})_2][\text{ReO}_4]$ but might still be attributed to Van Vleck paramagnetism that arises because the valence band is associated with the nearly degenerate a_{1u}, a_{2u} HOMO set of the macrocycles.

Conclusions

$[\text{Pd}(\text{tmp})_2][\text{ReO}_4]$ is isostructural with $[\text{Ni}(\text{tmp})_2][\text{ReO}_4]$ and $[\text{Cu}(\text{tmp})_2][\text{ReO}_4]$. All three of these semiconductors are ligand-oxidized and possess conduction bands formed from porphyrin $p-\pi$ orbitals. The ESR measurements confirm the tmp ligand as the site of oxidation. Because the conduction band arises from overlap of the porphyrin orbitals, the room-temperature conductivity is comparable with that of the best Pt–spine conductors, despite the fact that the interplanar separation (≈ 3.38 Å) is considerably longer than the Pt–Pt distance (~ 2.95 Å) in the Pt–spine conductors.

Acknowledgment. This work was supported by the Northwestern University Materials Research Center, NSF Grant DMR-8821571.

Registry No. $[\text{Pd}(\text{tmp})_2][\text{ReO}_4]$, 133042-93-0; $\text{Pd}(\text{tmp})$, 67159-01-7; $[\text{N}(\text{n-Bu})_4]\text{ReO}_4$, 16385-59-4; Pt, 7440-06-4.

Supplementary Material Available: Complete crystallographic details (Table IS), intramolecular bond distances and angles (Table IIIS), and best-weighted least-squares planes (Table IVS) (5 pages); $10|F_o|$ vs $10|F_c|$ data (Table IIS) (10 pages). Ordering information is given on any current masthead page.

Contribution from the Anorganisch-chemisches Institut der Technischen Universität München, D-8046 Garching bei München, Germany

Multiple Bonds between Main-Group Elements and Transition Metals. 91.¹ High-Oxidation-State Rhenium Complexes Containing the Hydridotris(1-pyrazolyl)borato Ligand

Ian A. Degan,[†] Joachim Behm,[‡] Malcolm R. Cook,[§] and Wolfgang A. Herrmann*

Received October 19, 1990

The rhenium(VII) complex $[\text{HB}(\text{pz})_3]\text{ReO}_3$ (1) is readily reduced by triphenylphosphine in the presence of excess $(\text{CH}_3)_3\text{SiX}$ ($X = \text{Br}, \text{Cl}$) to give the corresponding rhenium(V) complexes $[\text{HB}(\text{pz})_3]\text{ReOX}_2$ (2, $X = \text{Cl}$; 3, $X = \text{Br}$, $\text{pz} = \text{pyrazolyl}$ ($\text{C}_3\text{H}_3\text{N}_2$)). $[\text{HB}(\text{pz})_3]\text{ReOCl}_2$ (2), which seems to exist as two bond stretch isomers, reacts with 1 equiv of thiophenol in refluxing THF in the presence of a base [DBU or $\text{N}(\text{C}_2\text{H}_5)_3$] to give $[\text{HB}(\text{pz})_3]\text{ReO}(\text{Cl})(\text{SC}_6\text{H}_5)$ (4). Two equivalents of thiophenol reacts with 2 in refluxing THF, also in the presence of base, to give $[\text{HB}(\text{pz})_3]\text{ReO}(\text{SC}_6\text{H}_5)_2$ (5). 2 will react with 1,2-ethanedithiol or 1,2-benzenedithiol under similar conditions to give $[\text{HB}(\text{pz})_3]\text{ReO}(\text{S}_2\text{C}_6\text{H}_4)$ (6) and $[\text{HB}(\text{pz})_3]\text{ReO}(\text{S}_2\text{C}_2\text{H}_4)$ (7), respectively. The solid-state structures of 4 and 5 have been determined by X-ray crystallography. Both were found to be monomeric with an approximately octahedral arrangement of ligands around the rhenium atoms. 4 crystallizes in the orthorhombic space group $Pbca$ (No. 61) with cell parameters $a = 13.159(1)$ Å, $b = 18.656(1)$ Å, $c = 15.902(1)$ Å, $V = 3904(1)$ Å³, $Z = 8$, $R = 0.043$, and $R_w = 0.031$ for 2713 reflections with $I > 2\sigma(I)$. 5 crystallizes in the monoclinic space group $P2_1/c$ (No. 14) with cell parameters $a = 15.594(3)$ Å, $b = 21.624(1)$ Å, $c = 15.931(1)$ Å, $\beta = 107.00(1)^\circ$, $V = 5137(1)$ Å³, $Z = 4$, $R = 0.050$, and $R_w = 0.036$ for 6683 reflections with $I > 2\sigma(I)$.

Introduction

Recently we reported the synthesis and solid-state structure of the complex $[\text{HB}(\text{pz})_3]\text{ReO}_3$ (1).² This is a rare example of a rhenium(VII) compound containing the hydridotris(1-pyrazolyl)borato ligand. The only other rhenium(VII) example is the hexahydro complex $[\text{HB}(\text{pz})_3]\text{ReH}_6$.³ Two rhenium(V) complexes have also been reported, $[\text{HB}(\text{pz})_3]\text{ReOCl}_2$ and $[\text{HB}(\text{pz})_3]\text{ReSCl}_2$.^{4,5} 1 is particularly interesting, as it is an analogue

of $(\eta^5\text{-C}_5\text{Me}_5)\text{ReO}_3$, which has been shown to have a wide and varied chemistry and has been used as a starting material in the preparation of a great many high-oxidation-state rhenium com-

- (1) Part 90: Herrmann, W. A.; Watzlowik, P.; Kiprof, P. *Chem. Ber.*, in press.
- (2) Degan, I.; Herrmann, W. A.; Herdtweck, E. *Chem. Ber.* **1990**, *123*, 1347.
- (3) Hamilton, D. G.; Luo, X.-L.; Crabtree, R. H. *Inorg. Chem.* **1989**, *28*, 3198.
- (4) Abrams, M. J.; Davison, A.; Jones, A. G. *Inorg. Chim. Acta* **1984**, *82*, 125.
- (5) Duatti, A.; Tisato, F.; Refosco, F.; Mazzi, U.; Nicolini, M. *Inorg. Chem.* **1989**, *28*, 4564.

[†] Postdoctoral Fellow of the Royal Society, London.

[‡] Fellow of the Hanns-Seidel-Stiftung e. V., München.

[§] SERC/Royal Society NATO Postdoctoral Fellow.